JJEE

Volume 12 | Number 1 | March 2026 | Pages 138-151

Jordan Journal of Electrical Engineering

ISSN (print): 2409-9600, ISSN (online): 2409-9619

Homepage: jjee.ttu.edu.jo

Transient Behaviour Analysis of Wind Turbine Grounding Protection System

Abdelbari Younes[1*], Abdenbi Mimouni[2]

[1, 2] Laboratory of Electrical Engineering and Plasmas, Univ. Tiaret, Algeria
E-mail: Younes.abd@univ-tiaret.dz

Received: Aug 28, 2025 *Revised: Dec 23, 2025* *Accepted: Dec 23, 2025* *Available online: Mar 19, 2026*

***Abstract*—** Among the main sources of sustainable energy, wind power has established itself as a symbol of clean renewable energy. However, the installation of wind turbines in windy regions, where lightning strikes are more frequent, has led to growing concerns about their vulnerability to lightning storms. With the rapid expansion of wind farms, attention is increasingly focused on the intrinsic vulnerability of turbines to power surges generated by lightning strikes. With this in mind, this article proposes a comparative transient analysis of four distinct grounding system architectures (designated A, B, C, and D), examined under the influence of two levels of soil resistivity, using RLC equivalent pi-circuit modeling implemented in the MATLAB/Simulink environment. Unlike simplified study diagrams, our approach is distinguished by the representation of each individual conductor using an equivalent pi circuit, which allows us to understand the entire dynamic response of the device to high-frequency transient stresses. It was shown that, in a 2x2 star configuration (model D), the transient impedance values increased compared with other models. Simulation data also confirms that model D has a transient potential value of 70 kV. While model A compact 1x1 grid, has a value of 160 kV for a resistivity of 550 Ωm. In addition, by understanding the critical factor of resistivity, a cost-benefit analysis was used to determine that Model D was the most appropriate configuration of all, as it would reduce material costs while providing effective lightning protection.

***Keywords*—** Lightning protection system (LPS); Grounding system; Transient impedance; Lightning; Wind turbine.

1. INTRODUCTION

As fuelled by a growing demand for sustainable environmentally friendly energy, the scale of wind energy installations and the dimensions of wind turbines have expanded considerably over the last few decades. As wind energy expands worldwide at an unprecedented rate, lightning strikes on wind turbines have become a huge challenge [1, 2]. In recent years, manufacturers and particularly operators of wind turbines have been faced with a sharp rise in the costs of lightning damage, casting a shadow over the industry's rapid ascent. Insurance companies covering major wind farms have found that a significant proportion of their claims are due to lightning damage of the wind turbines blades [3]. When lightning strikes a wind turbine, it releases a powerful current that travels through the blades and tower to the earthing system and causes a spike in the earth potential. It is therefore essential to analyse the transient behaviour of wind turbines during such strikes to ensure the safe and reliable operation of wind energy installations and preserve their vital role in the renewable energy sector [4, 5].

To study the phenomenon of lightning-induced over voltages in wind turbines, researchers have historically used two main approaches: experiments on scale models and

* Corresponding author
DOI: https://doi.org/10.5455/jjee.204-1756372965

numerical simulations. Researchers are increasingly resorting to model experiments, a method that accurately reproduces the real transient impacts of lightning [6, 7]. For example, a scale of 3/100 replica of real wind power generation system has been used in both analytical and experimental studies of lightning surges, as reported in reference [8, 9]. Although these approaches offer physical validation of the phenomena, they are costly, complex to implement and limited by scale constraints. Compared to experimental approaches, numerical simulations offer a superior alternative for the assessment of wind turbine lightning transients, combining remarkable flexibility with exceptional accuracy to shed light on the complex dynamics of these powerful electrical events [10, 11]. The works carried out confirmed the reliability of a proposed numerical simulation technique for calculating lightning transient over voltages in.

Beyond the receptors and down conductors, the grounding system stands as the cornerstone of a wind turbine's lightning protection framework. It safely conducts lightning and fault currents to ground in order to prevent power surges. It also avoids dangerous potentials that could damage turbine components or endanger the lives of nearby people. To design a reliable earthing system, it is crucial to take local conditions into account, analyse the risks of short circuits and comply with international standards and national laws in force. The earthing system is often modelled as a resistive element, with its reactive components generally neglected at high frequencies [9, 10, 12-15]. This approach allows simplified yet robust modelling to guarantee the integrity of the wind turbine. In wind farms with interconnected turbine earthing systems, the reactive component dominates at lightning frequencies, requiring careful design [16]. To capture this complexity, more sophisticated models such as the representation of a conductor by a π-equivalent RLC circuit, have been proposed to simplify the representation of the complex response of the earthing system to the dynamic overvoltage of lightning [17].

Despite advances in the modelling of lightning transients, there is still a need for a systematic and comparative analysis of the different configurations of earthing systems under the dynamic impact of lightning. This study proposes a transient analysis technique that differs from previous work in that it involves integrated and complex modelling of the earthing system. We unveil a transient analysis technique that integrates the high-frequency characteristics of the lightning current into the grounding model in a complex way. Unlike simplified approaches, our model represents each horizontal conductor, electrode and vertical rod of the grounding system is modelled as a π-equivalent RLC circuit [17], thus capturing the full dynamic response of the system. In addition, we are carrying out a systematic comparative analysis of four distinct geometric configurations of earthing systems (compact and star grids) under two levels of ground resistivity (550 Ωm and 1000 Ωm). This analysis provides quantifiable data and clear recommendations on the optimal configuration. Finally, we quantify the impact of the geometry of the earthing system (number of meshes and position of the point of impact) on voltage and impedance transients, providing concrete evidence of the importance of physical design for safety and performance.

The dependent current sources within the network are articulated by a double exponential function, allowing realistic simulation of the lightning surge. Once the lightning current source has been defined, the transient potentials at the turbine ground terminals are accurately calculated. The renowned MATLAB computer software suite is being employed to solve the nodal equations, illuminating the transient behaviour of the wind turbine.

This paper is structured as follows. Section II sets out the modelling description. Section III shows simulation findings and discussions as well as the potential transients for different

types of grounding systems. Finally, some conclusions drawn from the present work are presented in Section IV.

2. LITERATURE REVIEW

2.1. Standards and Acceptable Limits

In order to guarantee the reliability and safety of wind turbine earthing systems, it has been necessary to design them in accordance with the latest international standards. These standards are as follows IEC 61400- 24:2010 (Lightning protection of wind turbines)[18], and IEEE Std 2760-2020 (Guide for the Design of Wind Farm Grounding Systems) [19].

These specifications define a minimum standard for lightning protection and earth potential. It should be noted that in this article the low frequency static earth impedance is a key factor. The current aim as described in these guides, is to keep the impedance value of the earthing system below 10 Ohms to ensure adequate dissipation of fault and lightning currents [20]. However, transient analysis reveals that impulse impedance (at high frequency) is the critical factor for overvoltage. The standards also define strict safety criteria based on the maximum acceptable touch and step voltages to prevent risks to personnel and damage to sensitive equipment. Our comparative analysis of configurations aims to identify the one that most effectively minimizes transient impedance, thereby ensuring that generated overvoltages remain within the safety limits defined by these standards.

2.2. Comparative Analysis of Existing Work

To highlight the contribution of this work, Table 1 presents a critical comparison of our approach with previous relevant studies in literature.

Table 1. Critical comparison of existing literature and the contribution of this work.

Study representative	Main model	Type of analysis	Lens main	Filled by our work
Ref. [12]	Resistive (Static)	Low Frequency	Determination of static earth resistance	We focus on the impedance transient (high frequency) critical for the lightning strike
Ref. [16], [20]	RLC/Pi-Equivalent	Transitory	Study of the effect of interco – nnections and the component reactive.	We provide a comparative systematic analysis of four geometries and a mathematical justification of the optimal configuration.
Ref. [21], [22]	Optimisation/Cost	Low Frequency /Static	Minimisation of the cost of materials for a target resistance	We integrate the Cost-benefit analysis into as a function of the transient performance (reduction of overvoltage) and not only of the static resistance.

3. MODELLING DESCRIPTION

3.1. Detailed Conductor Modeling and Hypotheses

The model adopted for the grounding conductor is based on the Transmission Line Model (TLM), whose RLC pi-equivalent circuit is a valid and widely used approximation for the analysis of lightning transients in commonly used simulation software like MATLAB/Simulink [23]. This model allows for the capture of the dynamic effects of the soil and the conductor at high frequencies.

Each segment of conductor is characterised by its parameters distributed per unit length: resistance (R), inductance (L) and capacitance (C). The L and C elements represent the parasitic elements (inductive and capacitive) of the buried conductor, which are essential for the transient analysis [24]. These parameters depend on the geometry of the conductor (diameter, length) and the electromagnetic properties of the soil, i.e. its resistivity and permittivity. The basic assumptions of this modelling are as follows:

1. Homogeneous soil: the resistivity and permittivity properties of the soil are assumed to be homogeneous. This simplifies the calculation of RLC values.
2. Linear behaviour: the components of the RLC circuit are modelled as linear and independent of current, which is a reasonable approximation for a lightning transient.
3. Validity of the model: the pi equivalent model has been shown to be valid for lightning wave frequencies in order to simulate surges correctly.

3.2. Equivalent Circuit of the Wind Turbine and The Grounding System

The adopted approach consists of modelling the blade's internal conductor as a surge impedance, called z_{blade} in Eq. (1) (as depicted in Fig. 1). This method aims to capture the lightning wave's reflections with precision. To simplify the circuit analysis, the blade is assumed to be oriented horizontally relative to the ground, simplifying the intricate dynamics of the storm's electric surge.

At the same time, the tower of the wind turbine and the grounding network are also represented as surge impedances, developed from simplified models inspired by transmission line structures. The tower impedance z_{tower} in Eq. (2) is calculated by modeling the structure as a vertical cylinder column having a height h and diameter r, capturing its dynamic behavior under lightning strikes. For the grounding system, its impedance z_{ground} is computed using multiple configuration approaches (Fig. 2), following the methodology presented in reference [25]. Configuration A is represented by a compact 1 × 1 grid, while configuration B takes the form of a 1 × 1 - star grid. Configuration C adopts a wider 2 × 2 grid, and configuration D reproduces it as a 2 × 2 - star grid. Each of these complex designs is distilled into a simplified equivalent RLC circuit, as indicated in Eqs. (3) to (5) [26].

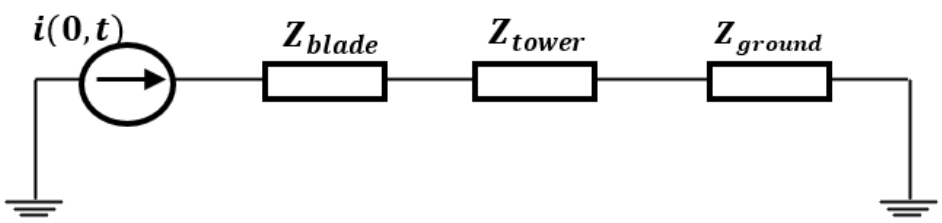

Fig. 1. Equivalent circuit of the wind turbine.

Figure 3 shows a transmission system with the blades and tower to the basic earthing system (A compact 1 × 1 grid). The Figure shows all the MATLAB blocks used in our simulation and the link between them. A lightning surge of 30 kA was induced on the system, and the resulting simulation was carried out using MATLAB Simulink software.

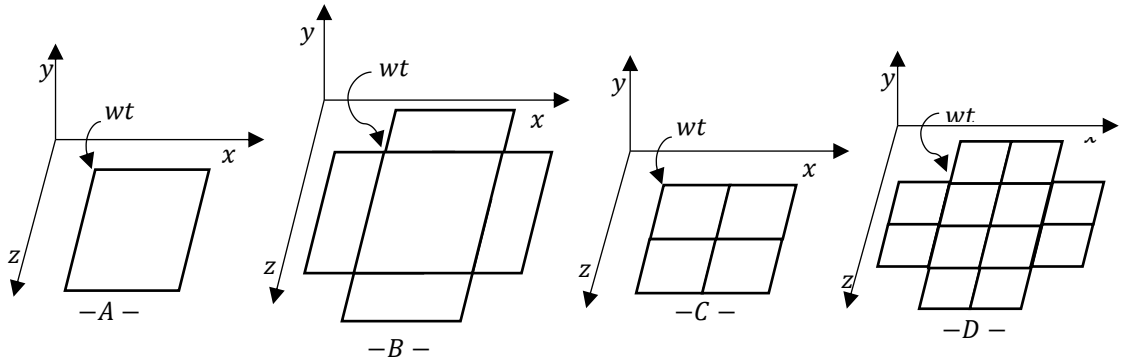

Fig. 2. Grounding grid buried in the soil.

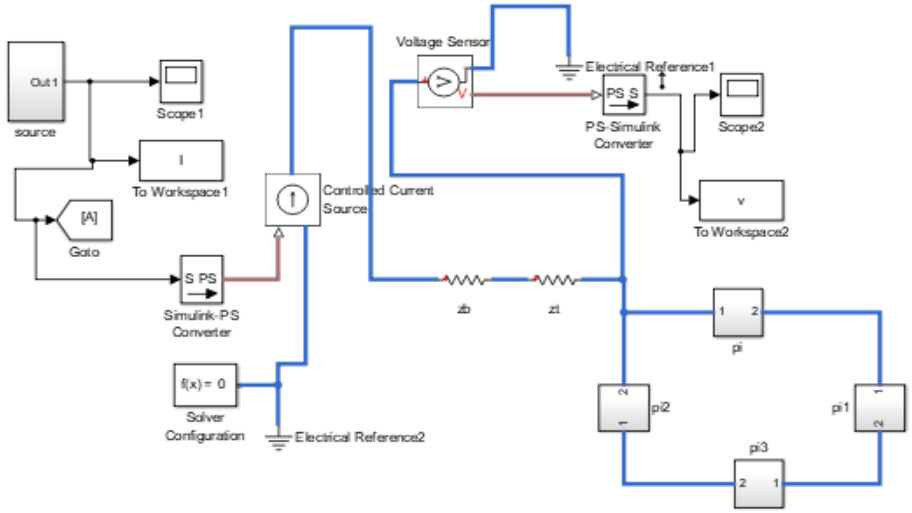

Fig. 3. Equivalent circuit in MATLAB Simulink.

The wind turbine's electrical behavior is represented through an equivalent transmission line circuit model, providing precise simulation of its dynamic response to electrical surges [27].

$$z_{blade} = 60(ln\frac{2\times L_b}{r_b}) \quad (1)$$

$$z_{tower} = 60(ln\frac{\sqrt{2}h}{r}) \quad (2)$$

where [3]:

L_b is the conductor's length in the turbine blade, measuring 43 m.

r_b represents the conductor's radius within the turbine blade, measuring 5 mm.

h is the Tower height, measuring 80 m.

r represents Tower radius, measuring 4.5m.

The constant resistance of a network is expressed by the equation provided, which is based on the principle of a regular flow of current through its structure [28]:

$$R = \frac{\rho}{2.\pi.l}\left[\ln\left(\frac{8.l}{d}\right) - 1\right] \quad (3)$$

The network capacity is calculated using the formula below, quantifying its electrical stability [28]:

$$C=\frac{2.\pi.\varepsilon_r.\varepsilon_0.l}{\ln\left(\frac{4.l}{d}\right)} \quad (4)$$

The permanent inductance of a grid is expressed by the equation below [28]:

$$L=2.10^{-7}.l.\ln\left(\frac{4.l}{d}\right) \quad (5)$$

The symbols are defined as follows:

ρ is soil resistivity. It is measured in (Ωm)

d is diameter of the electrode. It is measured in (m)

l represents the length of the electrode in (m).

ε_r is permittivity of soil in (farads/meter).

3.3. LIGHTNING CURRENT WAVEFORMS

In these models, the lightning current is represented by a double exponential function [18]:

$$i(t) = I_0(e^{-at} - e^{-bt}) \quad (6)$$

where, I_0, a and b are the variables that define the current peak, the rise time and the decay time, see Table 2, and Fig. 4.

Table 2. Parameters of the bi-exponential functions [18].

I_0 (KA)	33.7
a (s^{-1})	9.2×10^3
b (s^{-1})	4×10^5

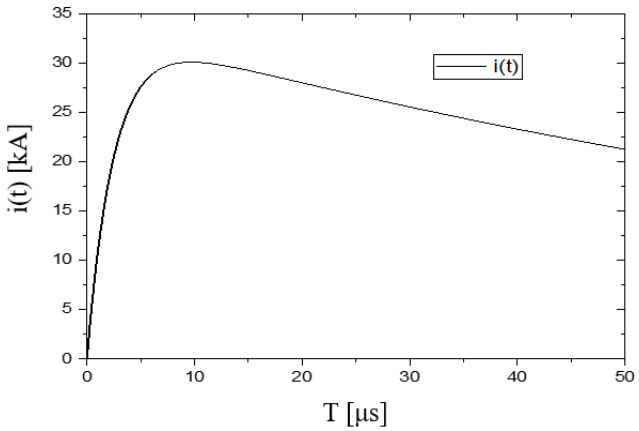

Fig. 4. Typical current waveform simulated by a double exponential equation.

3.4. Mathematical Articulation of the 2x2 Star Configuration Performance

The superior performance of the 2x2 star configuration (Model D) is justified by a mathematical derivation based on the Transmission Line Model (TLM) [23, 24] . The transient impedance $Z_{arm}(s)$ of a single radial arm, viewed from the injection point, is approximately given by $Z_{arm}(s) \approx Z_c \times coth(\gamma L)$, where Z_c is the characteristic impedance and γ is the propagation constant. If you have four impedances (Z_1, Z_2, Z_3, Z_4) connected strictly in parallel. The general formula for parallel impedances is based on admittance.

$$\frac{1}{Z_{eq}} = \frac{1}{Z_1} + \frac{1}{Z_2} + \frac{1}{Z_3} + \frac{1}{Z_4} \quad (7)$$

If all impedances are identical ($Z = Z_1 = Z_2 = Z_3 = Z_4$), the formula is simplified to:

$$Z_{eq} = (Z/4) \quad (8)$$

The 2x2 star configuration is composed of four radial arms ($N = 4$) connected in parallel at the central injection point. The total transient impedance $Z_{star}(s)$ is therefore the equivalent impedance of these four arms in parallel:

$$Z_{star}(s) = (1/N) \times Z_{arm}(s) = (1/4) \times Z_{arm}(s) \quad (9)$$

By comparing this impedance to that of a simple single-arm configuration ($Z_{single}(s) \approx Z_{arm}(s)$), it is demonstrated that:

$$Z_{star}(s) = (1/N) \times Z_{single}(s) \quad (10)$$

This relationship proves that the transient impedance of the 2x2 star configuration is reduced compared to a single-arm configuration, all else being equal. Given that the overvoltage v_{surge} is directly proportional to the transient impedance ($v_{surge}(t) = Z_{transient}(t) \times I_{lightning}(t)$), this impedance reduction directly translates into a significant reduction in the overvoltage observed in the simulations, thus theoretically validating the superiority of Model D.

4. RESULTS AND DISCUSSIONS

4.1. Transient Analysis for the Four Model Configuration

Table 3 summaries all the electrical and physical properties used in simulation.

Table 3. Electrical and physical parameters of the grounding systems.

Grounding grid configurations	l(m)	d(mm)	ρ (Ωm)	ε_r
A, B	12	14	550	15
C, D	6	14	550	15
A, B	12	14	1000	15
C, D	6	14	1000	15

The variation of impulse impedance and voltage when changing the type of grounding system is illustrated in Figs. 5 and 6.

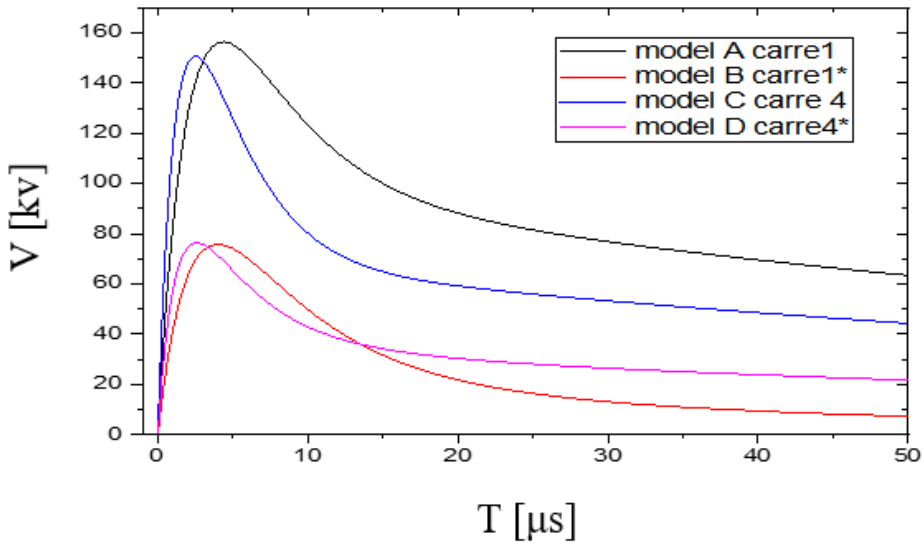

Fig. 5. Overvoltages for different grounding systems and for $\rho = 550\ \Omega m$.

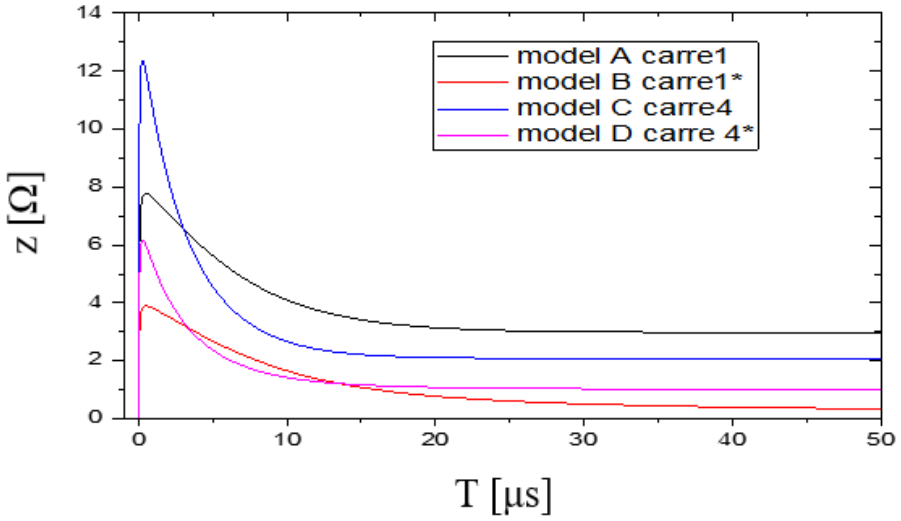

Fig. 6. Impedance for different grounding systems and for $\rho = 550\ \Omega m$.

From Fig. 5, it is evident that the four configurations studied as part of this investigation show rapid voltage surges. Each reaches its maximum voltage at roughly the same time range, suggesting a consistent timing for the peak voltage response to all configurations. Models A and C are characterised by high peak voltages 160 kv (model A) associated with more gradual decay. Models B and D, on the other hand, have lower peak voltages 70 kv (model B) and faster decay.

In Fig. 6, the impedance versus time (μs) shows distinct behaviour of the models. Each model has a distinct high peak near t=0 μs. The impedance then decreases rapidly, with model D stabilising fastest and model A slowest. All systems reach stable values between 0.5 Ω (model B) and 4 Ω (model A) after 25-40 μs, which shows different decay rates and stabilisation times.

Figure 7 shows that the voltage-time graph reveals much higher peaks, reaching several kilovolts, than in Fig. 5. Models A and C show imposing peaks with slow decay, while models B and D reach lower peaks and quickly fall back to minimum values, highlighting very marked contrasts in behaviour.

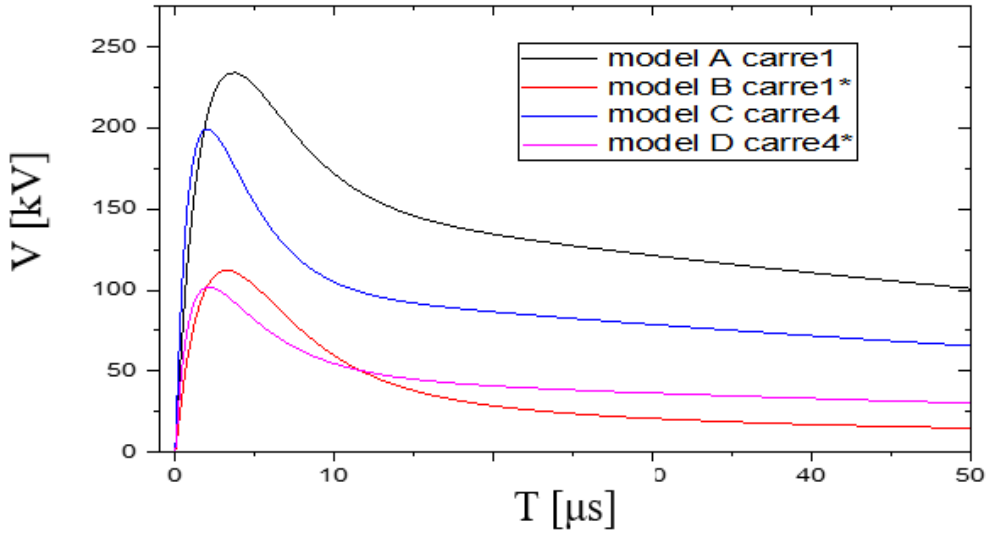

Fig. 7. Overvoltages for different grounding systems and for $\rho = 1000\ \Omega m$.

Figure 8 clearly shows the plot of impedance versus time, which reveals initial peaks near t=0 for four distinct systems, with models C and A reaching the highest peaks of around 20 Ω and 13 Ω, respectively. All the models show a sharp drop in impedance, followed by stabilisation at various value levels. Figure 8 is similar to Fig. 6, but for generally higher impedance values.

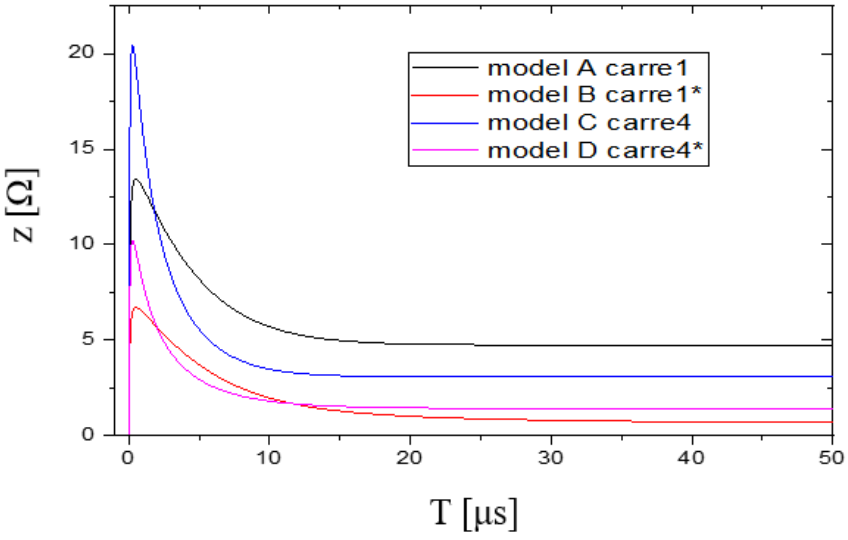

Fig. 8. impedance for different grounding systems and for $\rho = 1000\ \Omega m$.

4.2. Comparison of Transient Performance with New Wind Turbine Positions

This section examines the response of the system to variations in turbine positioning, as illustrated in Fig. 9, focusing on configurations C and D. This investigation reveals the effects of positional adjustments, providing a clear and concise understanding of their influence on the protection system.

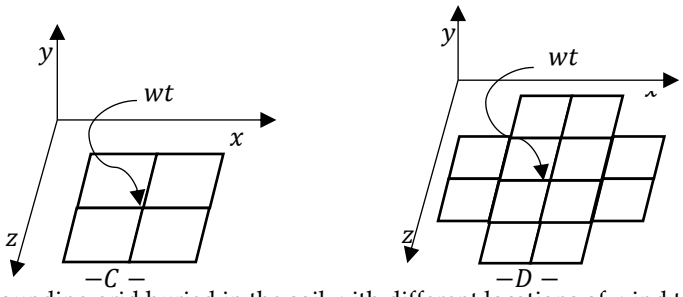

Fig. 9. Grounding grid buried in the soil with different locations of wind turbine.

The variation of voltage and impulse impedance for grounding grid configuration C and D when changing the position of wind turbine is illustrated in Figs. 10 and 11, respectively.

Similar to Fig. 5, Fig. 10 shows the same voltage pulse phenomenon (rapid rise and slow fall) on the same 50 μs time scale, observed for the wind turbine (WT) in the first position. The essential difference lies in the peak voltage amplitude and a final voltage at 50 μs which is lower in manipulation 2.

Figure 11 shows impedance versus time. Although all the curves show an initial impedance peak followed by stabilisation as in Fig. 6. The Figure represents the same systems but under different conditions that lead to lower overall impedances.

So, when the surge current is applied at the corner of the grid, the induced voltage and the impedance are the highest. In manipulation 2 with the increase in the number of return paths, the transient impedance has a very low value.

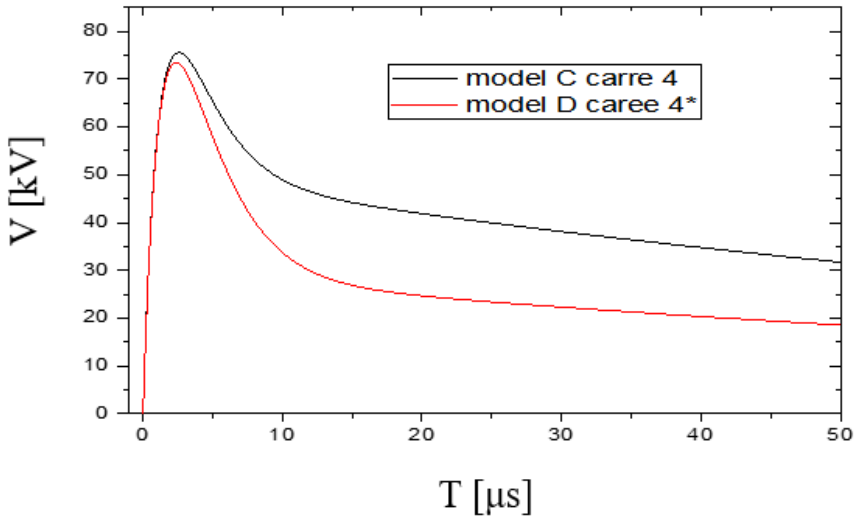

Fig. 10. Overvoltages for different WT locations and for $\rho = 550\ \Omega m$.

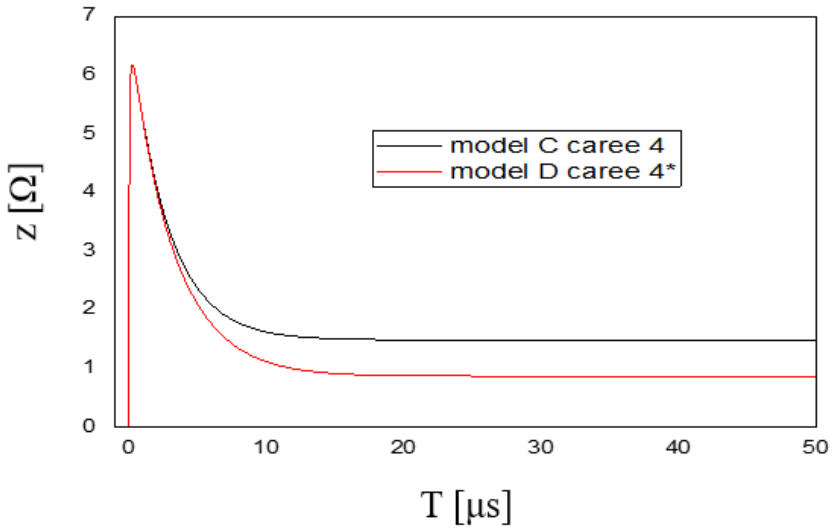

Fig. 11. impedance for different WT locations and for $\rho = 550\ \Omega m$.

4.3. Physical Interpretation and Implications

Analysis of Figs. 5 to 8 reveals marked contrasts between earthing configurations, which can be interpreted in terms of the physics of transients and the implications for lightning protection.

The Earthing System star models (B and D) show much lower transient earth potentials (70 kV for D at $\rho = 550\ \Omega m$) than the compact models (A and C, 160 kV for A). This difference results from a better distribution of the lightning current by the star configurations, reducing the transient impedance.

Model D's 56% reduction in maximum potential is crucial to minimising the risk of flashover and equipment damage. In addition, the rapid stabilisation of impedance in Models B and D ensures rapid energy dissipation, improving system resilience.

The increase in soil resistivity (Ωm) has a critical impact. Increasing the maximum transient earth potential from 550 Ωm to 1000 Ωm increases the maximum transient earth potential by 44% for model A (from 160 kV to 230 kV). This rise is due to the increase in ground impedance, impeding the flow of the lightning current.

The analysis of Manipulation 2 confirms that the impact at the corner of the grid (the most critical position) generates the highest voltages and impedances. This is attributed to the current concentration effect, highlighting the importance of the geometrical configuration and symmetry in minimising the transient earth potential.

4.4. Contextualization and Validation Against EMT Simulations

Although EMT (Electromagnetic Transients) simulation is recognised as the standard for transient simulation, the authors found that the application of an equivalent pi model was justified because of its recognised validity in lightning transients in known simulation software [29]. The results of this simulation are consistent with trends established in other EMT simulation studies, in particular for impulse impedance, which decreases with the complexity and size of the earthing system. The quantitative comparison of our results provides strong evidence of the relative effectiveness of the geometries studied. While it is recognised that full validation of this model using more complex EMT analyses would require further research, this model also provides accurate results.

4.5. Cost-Benefit Analysis

The adoption of a grounding configuration must be guided not only by technical performance but also by economic considerations. A Cost-Benefit Analysis (CBA) compares the relative cost of materials (primarily the total conductor length) for the configuration against its advantage in terms of protection (reduction of transient impedance) [21, 22].

The 2x2 star configuration (Model D) requires a longer conductor than Model A, resulting in a moderate cost in materials, as shown in Table 4. Nevertheless, it provides a reduction in transient impedance, which plays an important role in preventing overvoltages and the resulting material damage. As a result, Model D offers the best compromise of all, with a nominal increase in initial material costs that is offset by exceptional benefits in terms of protection performance. This further justifies, from an economic point of view, the adoption of the recommendations for a 2x2 star configuration.

Table 4. Critical comparison of existing literature and the contribution of this work.

Configuration	Total Conductor Length (Relative Cost)	Stabilized Transient Impedance (Performance)	Performance/Cost Ratio
C (1x1 grid)	L_c $(Reference)$	Z_c(High)	Low
D (2x2 Star)	$L_D \approx 2 \times L_c$	$Z_D \approx (1/2) \times Z_c$	High

L_c :represents the total side length of the square model C (Reference).
L_D:represents the total side length of the square model D.

5. CONCLUSIONS

This paper presents a technique to simulate the transient response of wind turbines following the lightning stroke. The obtained results show that soil resistivity and grid edge lengths for the grounding grid may affect the calculated value of the grounding impedance during the transient state of the wind turbine. Taking these factors into account, would help

to provide an efficient model of the grounding system under extreme lightning conditions and reduce the risk of lightning current in the lightning protection system for wind turbine. The simulation involved tested the four grounding systems for wind turbines with two different soil resistivity. It was observed that voltage and impedance vary significantly depending on the grounding system and soil resistivity. The findings show that the best grounding system is grounding model D (2x2 star grid) which appears as the best system. It has the ideal combination of low peak, low impedance and fast response in both soil resistivity. More precisely, model D reduces the maximum transient earth potential by 56% (from 160 kV to 70 kV) compared with model A (compact 1x1 grid) for a resistivity of 550 Ωm. This ensures optimal performance, with good voltage stability and high efficiency. Although this involves an increase in the number of conductors used compared with another configuration, this expense is offset by an improvement in transient impedance, which translates into long-term savings in maintenance costs.

The study also highlighted the critical influence of soil resistivity: an increase from 550 Ωm to 1000 Ωm resulted in a 44% increase in the maximum transient earth potential for model A, underlining the importance of a design adapted to local conditions. The position where the wind turbine is connected and the total number of meshes in the grid play an essential role in calculating the voltage and impedance transients. The peak voltage value reduces as the total number of conductors in the earthing grid increases. Taking these factors into account will help to provide an effective model of the earthing system under extreme lightning conditions and reduce the risk of lightning currents in the lightning protection system for wind turbines. The study of different new types of receivers for the blades or even the mechanical impact of the entire lightning protection system installed on the wind turbine that will be part of the project for our next research.

REFERENCES

[1] P. Ma, Y. Zhang, "Perspectives of carbon nanotubes/polymer nanocomposites for wind blade materials," *Renewable and Sustainable Energy Reviews*, vol. 30, no. C, pp. 651–660, 2014, doi: 10.1016/j.rser.2013.11.008.

[2] J. Zhang, Y. Han, L. Li, S. Feng, Z. Liao, "The impact of lightning strike to multi-blade on the lightning overvoltage and stresses of arresters in offshore wind farm," *IET Renewable Power Generation*, vol. 15, 2021, doi: 10.1049/rpg2.12206.

[3] A. Garolera, J. Holboll, S. Madsen, "Lightning transient analysis in wind turbine blades," International Conference on Power Systems Transients, 2013, https://orbit.dtu.dk/en/publications/lightning-transient-analysis-in-wind-turbine-blades

[4] A. Zalhaf, M. Ahmed, S. Ookawara, M. Abdel-Salam, "A Simplified model of wind turbine for lightning transient analysis as influenced by structure of grounding system," 5th International Conference on Electric Power and Energy Conversion Systems, 2018, pp. 1–6. doi: 10.1109/EPECS.2018.8443359.

[5] Q. Sun *et al.*, "Surge analysis for lightning strike on overhead lines of wind farm," *Electric Power Systems Research*, vol. 194, p. 107066, 2021, doi: 10.1016/j.epsr.2021.107066.

[6] M. Mamis, C. Keles, "ATP-EMTP simulation of lightning protection system for multi-storey building," *UNEC journal of engineering and applied sciences*, vol. 4, pp. 43–54, 2024, doi: 10.61640/ujeas.2024.0504.

[7] Y. Zhang, X. Zhang, "Statistic analysis of lightning transients on wind turbines," *Journal of Renewable and Sustainable Energy*, vol. 12, no. 6, p. 063302, 2020, doi: 10.1063/5.0031506.

[8] K. Yamamoto, T. Noda, S. Yokoyama, A. Ametani, "An experimental study of lightning overvoltages in wind turbine generation systems using a reduced-size model," *Electrical Engineering in Japan*, vol. 158, no. 4, pp. 22–30, 2007, doi: 10.1002/eej.20466.

[9] K. Yamamoto, T. Noda, S. Yokoyama, A. Ametani, "Experimental and analytical studies of lightning overvoltages in wind turbine generator systems," *Electric Power Systems Research*, vol. 79, no. 3, pp. 436–442, Mar. 2009, doi: 10.1016/j.epsr.2008.09.002.

[10] Z. Xiaoqing, "Calculation of transient potential rise on the wind turbine struck by lightning," *Scientific World Journal*, vol. 2014, p. 213541, 2014, doi: 10.1155/2014/213541.

[11] A. Zalhaf, M. Abdel-Salam, D. Mansour, S. Ookawara, M. Ahmed, "Assessment of wind turbine transient overvoltages when struck by lightning: experimental and analytical study," *IET Renewable Power Generation*, vol. 13, pp. 1360–1368, 2019, doi: 10.1049/iet-rpg.2018.5442.

[12] X. Zhang, Y. Zhang, C. Liu, "A complete model of wind turbines for lightning transient analysis," *Journal of Renewable and Sustainable Energy*, vol. 6, 2014, doi: 10.1063/1.4862204.

[13] W. Silva, W. Azevedo, A. Araujo, J. Filho, "Transient analysis of wind turbine grounding system: Comparison between interconnected overhead ground wire and underground bare conductor in wind farms," 37th International Conference on Lightning Protection, 2024.

[14] X. Zhang, Y. Zhang, "Calculation of lightning transient responses on wind turbine towers," *Mathematical Problems in Engineering*, vol. 2013, no. 1, p. 757656, 2013, doi: 10.1155/2013/757656.

[15] R. Rodrigues, V. Mendes, J. Catalão, "Lightning surges on wind power systems: study of electromagnetic transients," Electromagnetic Interference Issues in Power Electronics and Power Systems, 2011, doi: 10.2174/978160805240011101010096.

[16] M. Lorentzou, N. Hatziargyriou, B. Papadias, "Analysis of wind turbine grounding systems," 10th Mediterranean Electrotechnical Conference, 2000, doi: 10.1109/MELCON.2000.879686.

[17] W. Xiaohui, Z. Xiaoqing, Y. Dasheng, "An efficient algorithm of transient responses on wind turbine towers struck by lightning," *International Journal for Computation and Mathematics in Electrical and Electronic Engineering*, vol. 28, pp. 372–384, Mar. 2009, doi: 10.1108/03321640910929272.

[18] International Electrotechnical Commission, *Wind turbines. Part 24, Lightning protection*, 1st ed. Geneva, Switzerland: International Electrotechnical Commission, 2010, https://webstore.iec.ch/publication/19742.

[19] "IEEE Guide for Wind Power Plant Grounding System Design for Personnel Safety," *IEEE Std 2760-2020*, 2021, doi: 10.1109/IEEESTD.2021.9340101.

[20] A. Sunjerga, Q. Li, D. Poljak, M. Rubinstein, F. Rachidi, "Isolated vs. interconnected wind turbine grounding systems: effect on the harmonic grounding impedance, ground potential rise and step voltage," *Electric Power Systems Research*, vol. 173, pp. 230–239, Aug. 2019, doi: 10.1016/j.epsr.2019.04.010.

[21] J. Perng, Y. Kuo, S. Lu, "Grounding system cost analysis using optimization algorithms," *Energies*, vol. 11, no. 12, p. 3484, 2018, doi: 10.3390/en11123484.

[22] C. Silva *et al.*, "Methodology for optimizing electrical grounding grids in stratified soils using advanced calculation techniques and evolutionary algorithms," *Swarm and Evolutionary Computation*, vol. 95, p. 101953, 2025, doi: 10.1016/j.swevo.2025.101953.

[23] O. Gouda, G. Amer, T. El-Saied, "Factors affecting transient response of grounding grid systems," 5th International Multi-Conference on Systems, Signals and Devices, 2008, pp. 1–6. doi: 10.1109/SSD.2008.4632800.

[24] I. Gonos, M. Antoniou, I. Stathopulos, F. Topalis, "Transient analysis of the behaviour of grounding systems consisted by driven rods," https://www.semanticscholar.org/paper/Transient-analysis-of-the-behaviour-of-grounding-by-Gonos-Antoniou/1e3cf9867cdc4fa81f27400581eadfd0d5ed6052.

[25] T. Hara, O. Yamamoto, "Modelling of a transmission tower for lightning-surge analysis," *IEE Proceedings - Generation, Transmission and Distribution*, vol. 143, no. 3, pp. 283–289, 1996, doi: 10.1049/ip-gtd:19960289.

[26] L. Grcev, "Modeling of grounding electrodes under lightning currents," *IEEE Transactions on Electromagnetic Compatibility*, vol. 51, pp. 559–571, Sep. 2009, doi: 10.1109/TEMC.2009.2025771.

[27] A. Jiang, Z. Fu, Y. He, B. Wei, L. Wang, "Surge analysis of onshore wind farm due to multiple lightning strokes," *International Conference on Lightning Protection*, 2014, doi: 10.1109/ICLP.2014.6973293.

[28] M. Abdel-Salam, *High-Voltage Engineering: Theory and Practice*, New York: CRC Press Inc, 2000.

[29] R. Alipio, A. De Conti, F. Vasconcellos, F. Moreira, N. Duarte, J. Martí, "Tower-foot grounding model for EMT programs based on transmission line theory and Marti's model," *Electric Power Systems Research*, vol. 223, p. 109584, 2023, doi: 10.1016/j.epsr.2023.109584.